Gamma and pulsed electron radiolysis studies of CyMe<inf>4</inf>BTBP and CyMe<inf>4</inf>BTPhen: Identification of radiolysis products and

Citation for the original published paper (version of record):
Schmidt, H., Wilden, A., Modolo, G. et al (2021). Gamma and pulsed electron radiolysis studies of CyMe<inf>4</inf>BTBP and
CyMe<inf>4</inf>BTPhen: Identification of radiolysis products and effects on the hydrometallurgical separation of trivalent actinides and lanthanides. Radiation Physics and Chemistry, 189. http://dx.doi.org/10.1016/j.radphyschem.2021.109696

Radiation Physics and Chemistry 189 (2021) 109696

Contents lists available at ScienceDirect

Radiation Physics and Chemistry

journal homepage: www.elsevier.com/locate/radphyschem

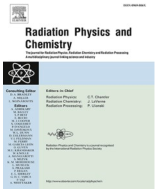

Gamma and pulsed electron radiolysis studies of CyMe$_4$BTBP and CyMe$_4$BTPhen: Identification of radiolysis products and effects on the hydrometallurgical separation of trivalent actinides and lanthanides

Holger Schmidt[a], Andreas Wilden[a,*], Giuseppe Modolo[a], Dirk Bosbach[a], Beatrix Santiago-Schübel[b], Michelle Hupert[b], Bruce J. Mincher[c], Stephen P. Mezyk[d], Jaroslav Švehla[e], Bohumir Grüner[e], Christian Ekberg[f]

[a] *Forschungszentrum Jülich GmbH, Institut für Energie- und Klimaforschung - Nukleare Entsorgung und Reaktorsicherheit- (IEK-6), 52428, Jülich, Germany*
[b] *Forschungszentrum Jülich GmbH, Zentralinstitut für Engineering, Elektronik und Analytik (ZEA-3), 52428, Jülich, Germany*
[c] *Idaho National Laboratory, Idaho Falls, ID, 83415, USA*
[d] *California State University at Long Beach, Department of Chemistry and Biochemistry, Long Beach, CA, 90840, USA*
[e] *Institute of Inorganic Chemistry, Czech Academy of Sciences, Hlavni 1001, 25068, Řež, Czech Republic*
[f] *Chalmers University of Technology, Nuclear Chemistry, Department of Chemical and Biochemical Engineering, 41296, Gothenburg, Sweden*

ARTICLE INFO

Keywords:
Nuclear waste treatment
Used nuclear fuel
Radiolysis
Solvent extraction
N-Donor extractants

ABSTRACT

The radiolytic stability of the highly selective ligands CyMe$_4$BTBP and CyMe$_4$BTPhen against ionizing gamma radiation was studied in 1-octanol solution. CyMe$_4$BTBP and CyMe$_4$BTPhen are important extractants for a potential treatment of used nuclear fuel. They were studied under identical experimental conditions to directly compare the effects of gamma and pulsed electron radiolysis on the ligands and systematically study the influence of structural changes in the ligand backbone. Distribution ratios of Am^{3+}, Cm^{3+} and Eu^{3+}, the residual concentration of CyMe$_4$BTBP and CyMe$_4$BTPhen in solution, and the formation of radiolysis products were studied as a function of absorbed gamma dose and presence of an acidic aqueous phase during irradiation. Quantitative and semi-quantitative analyses were used to elucidate the radiolysis mechanism for both ligands. Addition products of alpha-hydroxyoctyl radicals formed through radiolysis of the 1-octanol diluent to the ligand molecules were identified as the predominant radiolysis products. These addition products also extract trivalent metal ions, as distribution ratios remained high although the parent molecule concentrations decreased. Therefore, the utilization time of a solvent using these extractants under the harsh conditions of used nuclear fuel treatment could be considerably longer than expected. Understanding the radiolysis mechanism is crucial for designing more radiation resistant extractants.

1. Introduction

The hydrometallurgical treatment of used nuclear fuel is currently under investigation by several countries and international collaborative projects, as it may offer benefits in terms of resource savings and improved final disposal, and contribute to the sustainability of the nuclear fuel cycle and public acceptance (OECD-NEA, 2011; Veliscek-Carolan, 2016; Poinssot et al., 2016; Serp et al., 2017; Geist et al., 2020; Seidl et al., 2021). Detailed knowledge of the radiolytic degradation of organic ligands used in advanced processes for the hydrometallurgical treatment of used nuclear fuel is crucial for the design of these processes and their safe operation (Mincher and Mezyk, 2009; Mincher et al., 2009). As different organics are used in the processes (diluent, extractants, complexants, buffers, etc.), different degradation mechanisms, radiolytic vulnerabilities, sensitive functional groups and effects of additives need to be considered and understood. With this knowledge, modifications of the molecular structures can help protect these organic species against radiolytic degradation. Consequences of radiolytic ligand degradation are molecular alterations which may lead to changes in solvent properties (e.g. density, viscosity), separation effectiveness (affinity and selectivity), or formation of precipitates (Mincher et al., 2010a).

---

* Corresponding author.
E-mail address: a.wilden@fz-juelich.de (A. Wilden).

https://doi.org/10.1016/j.radphyschem.2021.109696
Received 30 April 2021; Received in revised form 22 June 2021; Accepted 30 June 2021

The group of BT(B)P-type nitrogen donor ligands is known to be highly selective for trivalent actinides (An(III)) over lanthanides (Ln (III)), and different members of this class of ligands have been used in different separation processes over the last decades (Veliscek-Carolan, 2016; Geist et al., 2020; Ekberg et al., 2008; Magnusson et al., 2009a; Panak and Geist, 2013; Wilden et al., 2013; Modolo et al., 2015; Geist and Panak, 2021). Kolarik et al. first suggested the use of 2,6-bis-(1,2,4-triazine-3-yl)pyridines (BTP-type ligands) for selective Am(III) extraction (Kolarik et al., 1999). After identifying the α-CH_2 position in the alkyl side-chain of the tested ligands to be the most vulnerable position, different branched and annulated modifications were synthesized and tested (Hill et al., 2002, 2005). $CyMe_4BTP$ (2,6-bis(5,5,8,8-tetra-methyl-5,6,7,8-tetrahydro-benzo[1,2,4]triazine-3-yl)pyridine) was found to have beneficial extraction properties with acceptable radiolytic stability (Hudson et al., 2006). However, due to the high An(III) distribution ratios, effective back-extraction of An(III) was problematic. Therefore, a second pyridine ring was added to the molecule backbone yielding 6,6′-bis(5,5,8,8-tetramethyl-5,6,7,8-tetrahydro-benzo[1,2,4] triazin-3-yl)[2,2']bipyridine ($CyMe_4BTBP$, Fig. 1), which showed very good extraction properties and stability (Geist et al., 2006). Therefore, the ligand was used in several European process demonstrations for the selective separation of An(III), like the r-SANEX (Modolo et al., 2013, 2014), 1-cycle-SANEX (Wilden et al., 2011, 2013; Modolo et al., 2014; Magnusson et al., 2013) and the CHALMEX processes (Aneheim et al., 2010, 2011, 2012a, 2013; Halleröd et al., 2015; Authen et al., 2021). The r-SANEX process has also been tested successfully on genuine spent fuel on the laboratory scale (Magnusson et al., 2009a). Similar to the BTP ligands, it was found that the radiolysis of BTBP ligands is induced in α-CH_2 positions of the side-chain, e.g. for the C5-BTBP ligand (Fermvik et al., 2009, 2010, 2011, 2012; Mincher et al., 2010b). Due to the linear alkyl substitutions, the C5-BTBP ligand was found to be very susceptible to radiolytic degradation, especially when aliphatic alcohols were used as diluent (Fermvik et al., 2009). Aliphatic alcohols are often used as diluents to increase the concentration of ligands that are only sparingly soluble in alkane diluents, or as phase modifiers to suppress third phase formation (Berthon et al., 2021; Geist and Modolo, 2009). The major radiolysis products were found to be α-oxidized C5-BTBP compounds with partially degraded C_5 chains. Due to the high excess of diluent molecules compared to extractant molecules, indirect radiolysis *via* a reaction with highly reactive species formed *in situ* by diluent radiolysis is most likely. This effect is referred to as sensitization effect (Sugo et al., 2002, 2007). The hydrolytic (Nicolas et al., 2011) and radiolytic stability of $CyMe_4BTBP$ was further studied in different chemical conditions (e.g. in different diluents) and for different irradiation conditions (i.e. alpha- and gamma irradiation, as well as electron- and ion-beam) and $CyMe_4BTBP$ was found to be sufficiently stable for its application in the hydrometallurgical treatment of used nuclear fuel (Halleröd et al., 2015; Retegan et al., 2007; Magnusson et al., 2009b; Aneheim et al., 2012b; Sulich et al., 2014).

Since An(III) extraction rates with the $CyMe_4BTBP$ ligand in 1-octanol are rather low and a phase-transfer agent (like DMDOHEMA (Geist et al., 2006) or TODGA (Modolo et al., 2008)) is needed to reach good extraction kinetics, further development was conducted. For metal complexation, the $CyMe_4BTBP$ ligand needs to rearrange from the thermodynamically preferred *trans*-conformation to the *cis*-conformation (Lewis et al., 2011, 2012, 2013). The *cis*-locked 2,9-bis(1,2,4-triazin-3-yl)-1,10-phenantroline ($CyMe_4BTPhen$, Fig. 1) ligand provides the required *cis*-conformation in a pre-organized molecular structure. Due to its preorganization, the complex formation is thermodynamically favored compared to $CyMe_4BTBP$ and the complexation is accelerated (Lewis et al., 2011).

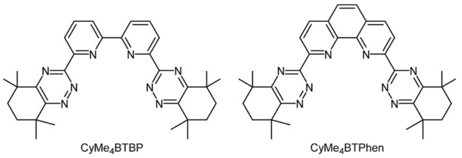

Fig. 1. Extractants investigated in this study: $CyMe_4BTBP$ (left) and $CyMe_4BTPhen$ (right).

The γ-radiolysis of $CyMe_4BTPhen$ has been investigated to a much lesser extent compared to $CyMe_4BTBP$ (Zhou et al., 2014; Distler et al., 2015; Kondé et al., 2016; Szreder et al., 2019; Zsabka et al., 2020). Distler and Kondé et al. investigated the radiolytic stability of $CyMe_4BTBP$ and $CyMe_4BTPhen$ in phenyl trifluoromethyl sulfone (FS-13) and $CyMe_4BTPhen$ in cyclohexanone diluents. They concluded that the stability of the extractant is higher in FS-13 compared to cyclohexanone-type diluents and that addition products of diluent radicals to the parent molecules are formed (Distler et al., 2015; Kondé et al., 2016). Zsabka et al. studied the radiolysis of $CyMe_4BTPhen$ in the ionic liquid tri-*n*-octylmethylammonium nitrate (Zsabka et al., 2020). Both groups observed increasing metal ion distribution ratios as a function of absorbed dose, assuming the formation of radiolysis products that are able to extract metal ions similar to the ligand itself.

In this study, we present comparative γ-radiolysis studies of the highly selective nitrogen donor ligands $CyMe_4BTBP$ and $CyMe_4BTPhen$ with respect to the extraction of Am(III), Cm(III), and Eu(III) with irradiated solvents as well as qualitative and (semi-)quantitative analyses of the solutions. The major radiolysis products are identified and (semi-)quantified as a function of absorbed dose, and the influence of the presence of nitric acid during irradiation is studied. This paper describes the results of collaborative work within the European projects SACSESS and GENIORS and collaborative work with US-DOE laboratories and should be understood as continuation of our previous work, where we investigated the effect of γ-radiolysis on the An(III)/Ln(III) separation *via* solvent extraction using $CyMe_4BTBP$ and $CyMe_4BTPhen$ in comparison (Schmidt et al., 2015, 2016).

2. Materials and methods

CAUTION: ionizing radiation and handling of radioactive material is hazardous. Refer to local safety precautions, legislation, and associated regulations. $CyMe_4BTBP$ and $CyMe_4BTPhen$ were purchased from Technocomm Ltd. (Wellbrae, Falkland, Scotland) and were used as received. Solutions of 10 mmol L^{-1} $CyMe_4BTBP$ or $CyMe_4BTPhen$ in 1-octanol (Merck, Darmstadt, Germany, analytical grade, >99%) were prepared and first irradiated under different conditions up to 413 kGy absorbed dose. In a later irradiation campaign, samples of $CyMe_4BTBP$ and $CyMe_4BTPhen$ in contact with 1 mol L^{-1} nitric acid were irradiated to higher doses of 622 kGy. The ^{60}Co γ-source at Chalmers University, Gothenburg, Sweden was used (Gamma cell 220, Atomic Energy of Canada Ltd.). Due to the radioactive decay of ^{60}Co, the provided dose rate decreased from 9.8 to 8.7 kGy h^{-1} during the experimental campaigns. Doses are reported relative to the initial dose rate determined using the ferric-cupric dosimeter without electron density corrections (Bjergbakke et al., 1970). The ferric-cupric dosimeter is used as standard technique at Chalmers, also taking into account the high dose-rate of the ^{60}Co γ-source. Samples of each ligand in 1-octanol solution were irradiated without, as well as in contact with nitric acidic solutions (Merck, Darmstadt, 65%, analytical grade, diluted with demineralized water (18.2 MΩ cm)) of different concentrations (0.1, 1.0 and 4.0 mol L^{-1} HNO_3). Organic phases were used without prior pre-equilibration. Equal volumes (1 mL) organic solvent and nitric acid were contacted during the irradiation experiments for which the samples were placed in the γ-source, until the calculated dose was reached. To avoid pressurization during the irradiation experiment, the screw caps were not closed tightly. Nevertheless, the samples are considered deaerated due to positive pressure generated by radiolysis. Small amounts of oxygen that may diffuse into the samples are continuously consumed by radiolysis. After removing the irradiated samples from the γ-source, phases were separated if necessary and the remaining organic phases were used for further analysis and solvent extraction experiments.

In the solvent extraction experiments 500 µL of the irradiated organic phase were contacted with 500 µL fresh 1.0 mol L^{-1} HNO_3 which was spiked with ^{241}Am (1.6 kBq), ^{244}Cm (1.6 kBq) and ^{152}Eu (2.8 kBq) tracer in 2 mL glass vials. The organic phases irradiated without contact to an aqueous phase or in contact with 0.1 and 4.0 mol L^{-1} HNO_3 were also directly contacted with 1.0 mol L^{-1} HNO_3 to avoid washing out degradation compounds. Radioactive tracers were purchased from Isotopendienst M. Blaseg GmbH, Waldburg, Germany, Oak Ridge National Laboratory, Oak Ridge, USA, and Eckert and Ziegler Nuclitec GmbH, Braunschweig, Germany. The vials were shaken vigorously for 90 min in a shaking device (2,500 rpm) at 22 °C to reach equilibrium. After centrifugation, the phases were separated, and aliquots of each phase were taken for analysis. Gamma spectroscopy was conducted using an HPGe (high-purity germanium) detector system purchased from EG & G Ortec, Munich, Germany, and equipped with the GammaVision software. The γ-lines at 59.5 keV and 121.8 keV were analyzed for ^{241}Am and ^{152}Eu, respectively. Alpha measurements were carried out for ^{241}Am (5486 keV) and ^{244}Cm (5805 keV) using an Ortec Octête-pc eight chamber alpha measurement system equipped with PIPS detectors. Sample preparation for alpha measurement was done by homogenizing a 10 µL alpha-spectroscopy sample in 100 µL of a mixture of Zapon varnish and acetone (1:100 v/v). This mixture was distributed over a stainless-steel plate obtained from Berthold, Bad Wildbad, Germany. The sample was dried under a heating lamp and annealed into the stainless-steel plate by a gas-flame burner. The results are reported as distribution ratios D, which were calculated by dividing the measured metal activity of the organic phase by the metal activity of the aqueous phase ($D = [M^{3+}{}_{org}]/[M^{3+}{}_{aq}]$). Given D values show an uncertainty of ±5% within the range of $0.01 < D < 100$. The minimum/maximum detectable distribution ratios were 0.002 and 500, respectively, due to the detection limits in either the organic or the aqueous phase.

Direct Infusion Mass Spectrometry measurements were performed using a Finnigan LCQ Fleet™ spherical Ion Trap LC/MS_n instrument (Thermo Scientific) at the Institute of Inorganic Chemistry, Rež, Czech Republic. All mass spectra were measured with APCI interface. 25 µL of the samples of initial concentration of the ligand were diluted to a volume of 1.0 mL with acetonitrile (for LC-MS, Aldrich, Gradient Grade). Mass Spectra from direct infusion by a syringe were measured with APCI in positive mode. Conditions used for APCI interface: Flow rate from a syringe infusion pump 10 µL min^{-1}; Sheath gas flow 15 L min^{-1}; Auxiliary gas flow 7 L min^{-1}; Source Voltage 3.75 kV; Vaporizer Temperature 400 °C; Capillary Temperature 250 °C; Capillary Voltage 48 V; Tube Lens Voltage 100 V and mass range from 50 to 2000.

Qualitative analyses for compound identification were performed using a hybrid linear ion trap FTICR (Fourier-Transform Ion Cyclotron Resonance) mass spectrometer LTQFT (Linear Tandem Quadrupole Fourier Transform) Ultra™ (Thermo Fisher Scientific, Bremen, Germany) coupled with an Agilent 1200 HPLC system (Agilent, Waldbronn, Germany). The mass spectrometer was first tuned and calibrated in the positive mode following the standard optimization procedure for all voltages and settings: Source Type: APCI; Source Voltage 6.00 kV; Capillary Voltage 34.00 V; Tube Lens Voltage 80.00 V; Capillary Temperature 275.00 °C; APCI Vaporizer Temperature 400.00 °C; Sheath Gas Flow 50.00 a.u.; Aux Gas Flow 5.00 a.u. Mass spectra were recorded in full scan from 100 to 1000 Da with a resolution of 100,000 at m/z 400. For the detection of radiolysis products, first a separation was carried out on the reversed phase column Zorbax Eclipse Plus C18 from Agilent (3.8 µm particles 100 × 4.6 mm) in a gradient run with solvent A (water with 0.1% formic acid) and solvent B (acetonitrile with 0.1% formic acid) as shown in Table 1. All data were processed using the XCalibur software version 2.0. For better visibility, peaks with an intensity >100,000 counts (which only occurred for the ligand molecules themselves) were cut off in all shown spectra to increase visibility of peaks with lower intensity (radiolysis products). All shown spectra are formatted to be directly comparable to each other. Only peaks with a relative threshold of >2% were analyzed. All spectra were collected using data of the HPLC runs from 3 to 13 min for $CyMe_4BTBP$ and from 0 to 18 min for $CyMe_4BTPhen$.

Table 1
Gradient used in the LC separation.

Time	Solvent A	Solvent B
0–2 min	40%	60%
2–10 min	Decrease to 2%	Increase to 98%
10–25 min	2%	98%
25–31 min	40%	60%

For quantitative mass spectrometric analyses, an HPLC-MS/MS method with APCI in positive ion mode was developed and validated using a Triple Quadrupole Qtrap6500 instrument (ABSciex, Darmstadt, Germany) coupled with an Agilent 1260 HPLC system (Agilent, Waldbronn, Germany) to quantify the concentrations of $CyMe_4BTBP$ and $CyMe_4BTPhen$ after irradiation. For $CyMe_4BTBP$, a Phenyl-X phase column from Thermo Scientific was used (2.6 µm particles, 100 × 4.6 mm) at 40 °C in an isocratic run with 95% methanol and 5% 5 mmol L^{-1} ammonium-acetate buffer at pH 6.5. Optimum separation performance for $CyMe_4BTBP$ was observed using a flow rate of 700 µL min^{-1} over 15 min. The reversed phase column Nucleodur C18 Gravity SB phase from Macherey&Nagel (3 µm particles, 150 × 4.6 mm) with an isocratic run (98% methanol and 2% water + 0.1% formic acid) at 40 °C, over 15 min, with a flow rate of 600 µL min^{-1} and an injection volume of 10 µL showed the best separation performance for $CyMe_4BTPhen$.

For the detection, the Multiple Reaction Monitoring (MRM) method was used with optimized method parameters for both ligands (Table 2). Mass spectrometer settings were: Curtain Gas 30 units; Gas 1 60 units; Gas 2 60 units; Temperature 350 °C; Needle Current (NC) 3 µA; Enhanced Potential 10 V. In all quantification experiments, data acquisition and processing were carried out using the software Analyst 1.6.1 (ABSciex, Darmstadt, Germany). For quantification the software Multiquant (ABSciex, Darmstadt, Germany) was used. The reproducibility for both ligands showed very good results with a variation coefficient ≤6%.

Pulse radiolysis experiments were conducted using the Laser-Electron Accelerator Facility (LEAF) at Brookhaven National Laboratory (NY, USA), which was described in detail by Wishart et al. (2004). For irradiation experiments, 1-octanol solutions of $CyMe_4BTBP$ or $CyMe_4BTPhen$ were irradiated and lifetimes of the generated solvated electron (e^-_{solv}) was observed in dependence of the ligand concentration, varying in the range from 2.5 to 10.0 mmol L^{-1} $CyMe_4BTBP$ or $CyMe_4BTPhen$, respectively. Additionally, the influence of nitric acid on e^-_{solv} absorbance by $CyMe_4BTPhen$ was tested in steady-state irradiation experiments using dried 1-octanol against 1-octanol contacted with 6.0 mol L^{-1} HNO_3, which yields an approximate organic HNO_3 concentration of 1.5 mol L^{-1} $HNO_{3,org}$ (Geist, 2010). Samples were irradiated in 1.00 cm Suprasil semimicro cuvettes sealed with Teflon stoppers. The doses per pulse for these experiments were in the range 40–60 Gy. Time-resolved kinetics were obtained using an FND-100 silicon diode detector and digitized using a LeCroy WaveRunner 640Zi oscilloscope

Table 2
Optimized reaction parameters for the ligand fragmentation.

Ligand	Fragment	Collision Energy	Cell Exit Potential	Declustering Potential
$CyMe_4BTBP$	m/z 535.1 to m/z 505.3	69 V	10 V	241 V
$CyMe_4BTBP$	m/z 535.1 to m/z 371.2	69 V	10 V	241 V
$CyMe_4BTPhen$	m/z 559.1 to m/z 529.3	67 V	6 V	200 V
$CyMe_4BTPhen$	m/z 559.1 to m/z 395.2	67 V	24 V	200 V

(4 GHz, 8 bit). Interference filters (10 nm bandpass) were used for the wavelength selection of the analyzing light (Mezyk et al., 2016).

3. Results and discussion

The radiolytic stability of the highly selective ligands CyMe$_4$BTBP and CyMe$_4$BTPhen was studied in parallel to compare the effects of radiolysis. 10 mmol L^{-1} solutions in 1-octanol were irradiated without contact to an aqueous phase, as well as in contact with 0.1, 1.0 and 4.0 mol L^{-1} HNO$_3$. After irradiation, phases were separated when needed and the irradiated solvent phases were further studied. ^{241}Am, ^{244}Cm and ^{152}Eu distribution ratios were determined in extraction experiments using fresh 1.0 mol L^{-1} HNO$_3$. Europium was used as a representative for trivalent lanthanides. Mass spectrometric analyses of the irradiated solvent phases were performed to identify the radiolysis products of the ligand molecules and to (semi-) quantify the remaining extractant and radiolysis product concentrations to investigate the radiolysis mechanism of both ligands. The radiolysis mechanism was further studied using pulsed electron radiolysis.

3.1. Solvent extraction

Fig. 2 shows the Am^{3+} and Eu^{3+} distribution ratios for CyMe$_4$BTBP and CyMe$_4$BTPhen as a function of absorbed dose. Curium was found to behave like americium under all tested conditions, with just slightly lower *D* values. Corresponding Cm data is shown in the Supplementary Information (Fig. S1). We found decreasing metal ion distribution ratios for both ligands as a function of absorbed dose when irradiated without contact to an aqueous phase. For CyMe$_4$BTBP the *D* values decreased quickly and the lower detection limit of the *D* values was reached within 200 kGy absorbed dose for ^{241}Am^{3+}. CyMe$_4$BTBP is a highly selective extractant for trivalent actinide ions (Geist et al., 2006), as indicated by the generally low *D* values measured for Eu^{3+} extraction. Therefore, the lower detection limit of the ^{152}Eu^{3+} *D* values was reached much earlier, within 100–150 kGy absorbed dose. CyMe$_4$BTPhen extracts trivalent metal ions with higher *D* values under the same conditions (Lewis et al., 2011). Therefore, all measured *D* values were generally higher compared to CyMe$_4$BTBP. Furthermore, the decrease in *D* values did not proceed uniformly. Instead, up to ca. 75 kGy absorbed dose, *D* values decreased quickly, while a much slower decrease was observed between 75 and 300 kGy. This behavior cannot be explained by a decrease in extractant concentration due to radiolysis alone. As we show below, some of the formed radiolysis products seem to be able to extract trivalent metal ions themselves. The stepwise reduction in *D* values for CyMe$_4$BTPhen could therefore be due to the build-up of a radiolysis product which also extracts trivalent metal ions, which is then prone to radiolytic degradation itself. The selectivity of the extractants in the solvent extraction experiments did not change much with increasing absorbed dose. Therefore, the radiolysis products also seem to be selective for trivalent actinide extraction.

During process operation, the organic solvent will be irradiated in contact with nitric acid solutions. Therefore, we tested the extraction of trivalent metal ions for solvents irradiated in contact with 0.1, 1, and 4 mol L^{-1} HNO$_3$ solutions. After irradiation, the phases were separated, and the irradiated organic phases were contacted with fresh 1 mol L^{-1} HNO$_3$ containing trace metal ions. These results are also shown in Fig. 2. Under most conditions, the observed distribution ratios were higher compared to the extraction series without addition of HNO$_3$ during

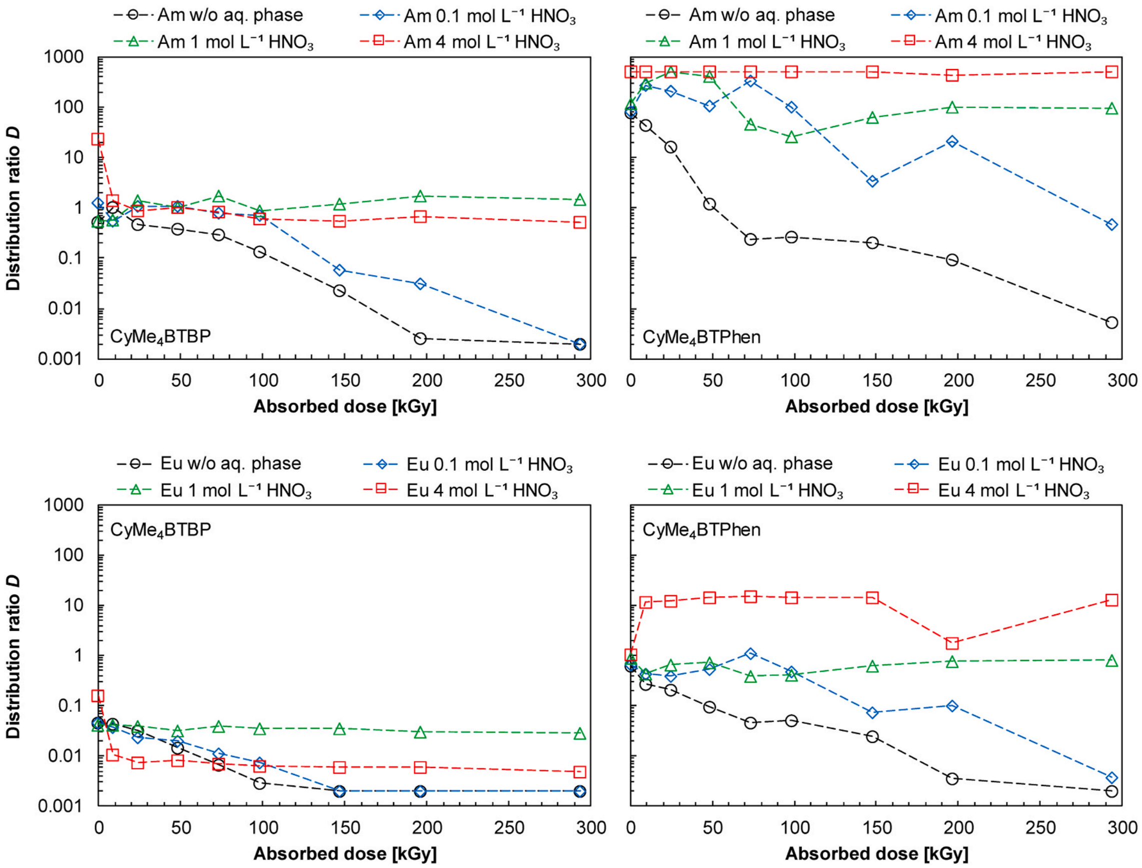

Fig. 2. Am^{3+} (top) and Eu^{3+} (bottom) distribution ratios as a function of absorbed dose for CyMe$_4$BTBP (left) and CyMe$_4$BTPhen (right). Extraction experiments after γ-irradiation of solutions of 10 mmol L^{-1} ligand in 1-octanol without and with contact to 0.1, 1.0 and 4.0 mol L^{-1} HNO$_3$. The solvent extraction experiments were conducted using the irradiated solvent phase and fresh 1.0 mol L^{-1} HNO$_3$ spiked with ^{241}Am, ^{244}Cm, and ^{152}Eu tracer. Given *D* values show an uncertainty of ±5% within the range of $0.01 < D < 100$.

irradiation, and the selectivity of the extractants remained high. The estimated annual dose to a solvent in used nuclear fuel treatment differs in the range 250 kGy to 125 MGy, depending on fuel type and burn-up (Fermvik et al., 2010; Magnusson et al., 2009b; Logunov et al., 2006). The results show that both ligands can be used in a continuous separation process for many extraction cycles, as the ligands will likely be used in contact with higher nitric acid concentrations during the extraction steps (where fission products with high gamma dose rate are present). The addition of 0.1 mol L^{-1} HNO_3 during irradiation caused a slower decrease of *D* values as a function of absorbed dose. For $CyMe_4BTBP$ the lower detection limit of the *D* values was reached after 300 kGy absorbed dose for $^{241}Am^{3+}$. For 1 and 4 mol L^{-1} HNO_3 the $CyMe_4BTBP$ *D* values remained relatively constant up to 300 kGy. Interestingly, the contact with 1 and 4 mol L^{-1} HNO_3 during irradiation caused increased *D* values for $CyMe_4BTPhen$. This is partly due to a slight co-extraction of nitric acid in the irradiated solvent, causing slightly higher equilibrium nitric acid concentrations in the extraction experiments. In the series irradiated in contact with 4 mol L^{-1} HNO_3, the Am^{3+} *D* values were very high over the whole range of absorbed doses studied. The Eu^{3+} *D* values increased at 10 kGy absorbed dose and remained almost constant for higher absorbed doses. The Am^{3+} *D* values of the series irradiated in contact with 1 mol L^{-1} HNO_3 first shows an increase of *D* values up to ca. 50 kGy, then a slight decrease between 50 and 100 kGy, and another increase up to 300 kGy. A comparable, but less pronounced behavior, was also observed for the Eu^{3+} *D* values. Such a behavior cannot be explained by the co-extraction of nitric acid. Instead, this behavior is likely explained by the formation of radiolysis products which can extract trivalent metal ions themselves, as described above. Similar behavior was observed for $CyMe_4BTPhen$ in FS-13 (Kondé et al., 2016), as well as $CyMe_4BTPhen$ in the ionic liquid tri-*n*-octylmethylammonium nitrate (Zsabka et al., 2020). A lower decrease in *D* values for solvents irradiated in contact with HNO_3 solutions was also observed for C5-BPP (2,6-bis(5-(2,2-dimethylpropyl)-1*H*-pyrazol-3-yl)pyridine, another highly selective N-Donor extractant) in a mixture of kerosene, 1-octanol and 2-bromohexanoic acid (Wilden et al., 2016). A clear statement towards the comparison of the radiolytic stability for the two extractants cannot be made based on the measured *D* values, as the initial *D* values already differ too much. Therefore, quantitative information on the extractant concentration as a function of absorbed dose using mass spectrometric methods is discussed below.

3.2. Identification of radiolysis products

Following the results of solvent extraction experiments, additional irradiation experiments were conducted to study the irradiated solvents using mass spectrometric techniques. Based on the extraction results, we decided to perform these experiments with solvents irradiated without contact to an aqueous phase and in contact with 1.0 mol L^{-1} nitric acid only. These two experimental conditions showed the most interesting results in the solvent extraction experiments, clearly indicating that changes in the $CyMe_4BTBP$ and $CyMe_4BTPhen$ molecular structures took place. The aim of the mass spectrometric measurements was to measure the extractant concentration in the irradiated solvents, as well as to identify and if possible, to semi-quantify the radiolysis products. Quantitative analyses were only possible for the parent $CyMe_4BTBP$ and $CyMe_4BTPhen$ molecules. For the radiolysis products no calibration standards were available and thus, a quantification was not possible. Instead, the measured intensities in the HPLC-MS spectra are discussed (semi-quantification). For the identification of radiolysis products, we used high resolution mass spectrometry (HR-MS) measurements with prior high-performance liquid chromatography (HPLC). Samples irradiated in contact with 1.0 mol L^{-1} nitric acid to moderate absorbed doses of ca. 100 kGy were most suitable for radiolysis product identification, as they included the parent molecules as well as the radiolysis products in enough quantities. Fig. 3 shows exemplary mass spectra of $CyMe_4BTBP$ and $CyMe_4BTPhen$ solutions irradiated to 132 kGy absorbed dose without contact to an aqueous phase. The mass spectra from all irradiated samples of both extractants irradiated without (10–413 kGy) or with (10–623 kGy) nitric acid contact are shown in the Supplementary Information (Figs. S2–S5). Nitric acid contacted samples were irradiated to higher doses, as the solvent extraction experiments suggested a protective effect and thus higher absorbed doses were necessary to result in notable degradation.

The peaks found at *m/z* 535.3291 and 559.3290 were assigned to the protonated $CyMe_4BTBP$ and $CyMe_4BTPhen$ species ($M+H^+$), respectively. The measured *m/z* ratios were in very good agreement with *m/z* ratios calculated from the proposed molecular formulae, as shown in Table 3 and Table 4. Sodiated species were detected at *m/z* 557.3113 and 581.3109 ($M+Na^+$), as sodium is widespread in glassware, solvents, and the mass spectrometer ion sources. The $CyMe_4BTPhen + Na^+$ species is better visible compared to the $CyMe_4BTBP + Na^+$ species, which

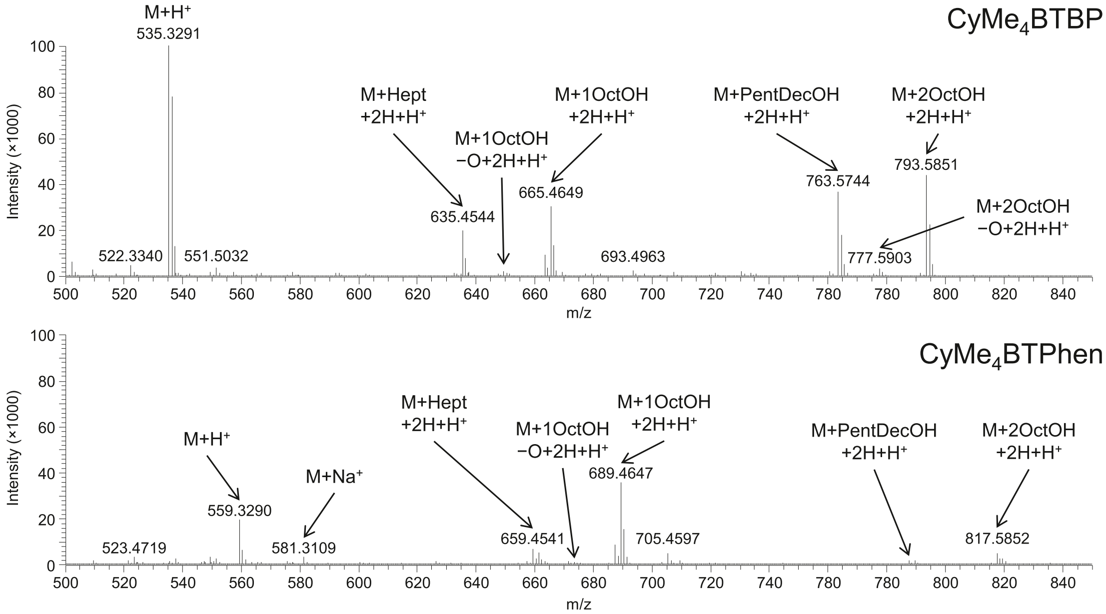

Fig. 3. Mass spectra of 10 mmol L^{-1} $CyMe_4BTBP$ (top) and $CyMe_4BTPhen$ (bottom) in 1-octanol irradiated to 132 kGy absorbed dose without contact to nitric acid. M = $CyMe_4BTBP$ or $CyMe_4BTPhen$, OctOH = α-hydroxyoctyl, PentDecOH = 8-hydroxypentadecanyl, Hept = heptyl.

Table 3

Overview of the identified species in irradiated $CyMe_4BTBP$ samples. *m/z* ratios were calculated using the given molecular formulae and compared to the measured *m/z* ratios.

M = $CyMe_4BTBP$, OctOH = α-hydroxyoctyl, PentDecOH = 8-hydroxypentadecanyl, Hept = heptyl.

$CyMe_4BTBP$ species	Measured *m/z* ratio	Calculated *m/z* ratio	Molecular formula
Dicarbonitrile	207.0665	207.0665	$C_{12}H_7N_4^+$
Carbonitrile	371.1979	371.1979	$C_{22}H_{23}N_6^+$
M + H^+	535.3291	535.3292	$C_{32}H_{39}N_8^+$
M + Na^+	557.3113	557.3112	$C_{32}H_{38}N_8Na^+$
M + Hept + H^+	633.4387	633.4388	$C_{39}H_{53}N_8^+$
M + Hept + 2H + H^+	635.4544	635.4544	$C_{39}H_{55}N_8^+$
M + 1OctOH − O + 2H + H^+	649.4700	649.4701	$C_{40}H_{57}N_8^+$
M + 1OctOH + H^+	663.4490	663.4493	$C_{40}H_{55}N_8O^+$
M + 1OctOH + 2H + H^+	665.4649	665.4650	$C_{40}H_{57}N_8O^+$
M + PentDecOH + H^+	761.5770	761.5589	$C_{47}H_{69}N_8O^+$
M + PentDecOH + 2H + H^+	763.5744	763.5745	$C_{47}H_{71}N_8O^+$
M + 2OctOH − O + 2H + H^+	777.5903	777.5902	$C_{48}H_{73}N_8O^+$
M + 2OctOH + H^+	791.5695	791.5694	$C_{48}H_{71}N_8O_2^+$
M + 2OctOH + 2H + H^+	793.5851	793.5851	$C_{48}H_{73}N_8O_2^+$

Table 4

Overview of the identified species in irradiated $CyMe_4BTPhen$ samples. *m/z* ratios were calculated using the given molecular formulae and compared to the measured *m/z* ratios. M = $CyMe_4BTPhen$, OctOH = α-hydroxyoctyl, PentDecOH = 8-hydroxypentadecanyl, Hept = heptyl.

CyMe4BTPhen species	Measured m/z ratio	Calculated m/z ratio	Molecular formula
Dicarbonitrile	231.0665	231.0665	$C_{14}H_7N_4^+$
Carbonitrile	395.1978	395.1979	$C_{24}H_{23}N_6^+$
M + H^+	559.3290	559.3292	$C_{34}H_{39}N_8^+$
M + Na^+	581.3109	581.3112	$C_{34}H_{38}N_8Na^+$
M + Hept + H^+	657.4385	657.4388	$C_{41}H_{53}N_8^+$
M + Hept + 2H + H^+	659.4541	659.4544	$C_{41}H_{55}N_8^+$
M + 1OctOH − O + 2H + H^+	673.4698	673.4701	$C_{42}H_{57}N_8^+$
M + 1OctOH + H^+	687.4491	687.4493	$C_{42}H_{55}N_8O^+$
M + 1OctOH + 2H + H^+	689.4647	689.4650	$C_{42}H_{57}N_8O^+$
M + PentDecOH + H^+	785.5587	785.5589	$C_{49}H_{69}N_8O^+$
M + PentDecOH + 2H + H^+	787.5745	787.5745	$C_{49}H_{71}N_8O^+$
M + 2OctOH − O + 2H + H^+	801.5907	801.5902	$C_{50}H_{73}N_8O^+$
M + 2OctOH + H^+	815.5696	815.5694	$C_{50}H_{71}N_8O_2^+$
M + 2OctOH + 2H + H^+	817.5852	817.5851	$C_{50}H_{73}N_8O_2^+$
M + 2OctOH + 4H + H^+	819.6016	819.6008	$C_{50}H_{75}N_8O_2^+$

occurs in smaller intensity below the label threshold limit in Fig. 3 (but still well measured). The most prominent radiolysis products found in the measured mass spectra were best described as addition products of the diluent 1-octanol. Longer chained alcohols are known to yield α-hydroxyalkyl radicals and other radiolysis products under irradiation (Mincher et al., 1994, 2010b; Freeman, 1970; Symons and Eastland, 1977; Swallow, 1987; Nilsson et al., 2006). The most important radiolysis reactions for longer chained alcohols are summarized in equations (1)–(4):

$$RCH_2OH + \gamma \rightarrow [RCH_2OH]^* \rightarrow e^-_{solv} + [RCH_2OH]^{\bullet +} \tag{1}$$

$$[RCH_2OH]^{\bullet +} \rightarrow RC^{\bullet}HOH + H^+ \tag{2}$$

$$H^+ + e^-_{solv} \rightarrow H^{\bullet} \tag{3}$$

$$RCH_2OH + H^{\bullet} \rightarrow RC^{\bullet}HOH + H_2 \tag{4}$$

The initial products formed during alcohol radiolysis are solvated electrons (e^-_{solv}) and the corresponding alcohol radical cations ($[RCH_2OH]^{\bullet +}$), Equation (1). The radical cations decompose to form α-hydroxyalkyl radicals (2). The solvated electron can react with protons to yield the hydrogen radical $H^{\bullet}$ (3) (Buxton et al., 1988). Hydrogen radicals commonly react with diluent molecules *via* hydrogen atom abstraction also resulting in the formation of carbon-centered α-hydroxyalkyl radicals (4). The α-hydroxyalkyl radicals can react with the ligand molecules with the formation of the observed addition products. The radiolysis products were identified as addition product with one or two of these α-hydroxyoctyl radicals (OctOH). The *m/z* ratios of the M+3OctOH+H^+ products were only found with very low intensities in a few samples. Interestingly, lower *m/z* ratios than the parent molecule masses were barely observed. The addition reaction with the α-hydroxyoctyl radical seems to be more probable than ligand degradation, at least for the investigated dose range of up to 623 kGy absorbed dose. This is partly explained by the relatively low concentration (0.01 mol L^{-1}) of $CyMe_4BTBP$ or $CyMe_4BTPhen$ compared to the diluent 1-octanol (ca. 6.4 mol L^{-1}, equals ca. 640 times higher concentration). Therefore, the radiolysis of diluent molecules is expected to be the preferred interaction of the incoming gamma rays producing the highly reactive diluent radicals. These diluent radicals then react with the ligand molecules, which is frequently referred to as indirect radiolysis (Mincher et al., 2010a). The reactivity of such diluent radicals depends on the nature of the diluent and was referred to as the sensitization effect (Sugo et al., 2002, 2007). Intensities of the different 1-octanol addition products decreased with the number of additions (see Fig. 3). The reaction of extractant molecules with diluent radicals was described previously by Fermvik et al. for the radiolysis of $CyMe_4BTBP$ in cyclohexanone and 1-hexanol (Fermvik, 2011), and by Wilden et al. for the radiolysis of C5-BPP (Wilden et al., 2016), a related nitrogen donor ligand. Zsabka et al. recently observed addition reactions of the cations of an ionic liquid to the $CyMe_4BTPhen$ ligand, as well (Zsabka et al., 2020).

We assume that the α-hydroxyoctyl radical addition reaction takes place *via* $H^{\bullet}$ atom abstraction from the parent molecules. This should yield addition products with *m/z* ratios of 663.4493 and 687.4493 in the protonated forms for the M+1OctOH addition products of $CyMe_4BTBP$ and $CyMe_4BTPhen$, respectively. However, both *m/z* ratios were only found at trace levels. Instead, *m/z* ratios with two and in some cases four mass units higher compared to the expected species were found predominantly. This could be explained by the additional reduction of one or two unsaturated bonds in the ligand molecules. This reduction is likely caused by reactions with reducing species (e.g. hydrogen radicals ($H^{\bullet}$) or H_2), formed by diluent radiolysis (cf. equations (3) and (4)) (Mincher and Mezyk, 2009). The yield of H_2 production by radiolysis is relatively high in alcohols, compared to other diluents (Swallow, 1987; Yu et al., 2010). The reduction of one C=C bond in the M+1OctOH molecule results in calculated *m/z* ratios of 665.4650 and 689.4650 (protonated form) for $CyMe_4BTBP$ and $CyMe_4BTPhen$, respectively (*m/z* ratios 665.4649 and 689.4647 in Fig. 3 labelled M+1OctOH+2H + H^+). Similar reduction products were observed for the addition of two α-hydroxyoctyl radicals and other addition products for both ligands. Fig. 3 shows that these reduced species were found predominantly.

Another possible route for the formation of addition products would be the initial reaction of an extractant with a solvated electron to form the extractant radical anion. This route was proposed by Szreder et al. (2019), showing that in addition to equation (3), the extended π-system of the ligand molecules should also be able to incorporate and stabilize the solvated electron (cf. equation (5)).

$$CyMe_4BTPhen + e^-_{solv} \rightarrow [CyMe_4BTPhen]^{\bullet -} \tag{5}$$

Yu et al. further reported the formation of *n*-heptane and pentadecan-8-ol (*via* addition of heptyl with α-hydroxyoctyl radicals) among others in ^{60}Co irradiated 1-octanol solution of up to 600 kGy absorbed dose (Yu et al., 2010). These products are also likely produced by radical reactions with the intermediate formation of the *n*-heptyl and 8-hydroxypentadecanyl radicals. We observed the corresponding addition products of the *n*-heptyl radical with *m/z* 633.4387 and 657.4385 of the protonated species for CyMe$_4$BTBP and CyMe$_4$BTPhen, respectively (Tables 3 and 4). Again, the reduced forms (*m/z* 635.4544 and 659.4541) were predominantly found. The 8-hydroxypentadecanyl radical addition products were found in their reduced form at *m/z* 763.5744 for CyMe$_4$BTBP under both conditions. For CyMe$_4$BTPhen, the unreduced form (*m/z* 785.5587) was mainly observed under acidic conditions, while the reduced form (*m/z* 787.5745) was predominantly formed in neat organic solution. Additionally, *m/z* ratios of addition products with −16 mass units (M+1OctOH−16, M+2OctOH−16) were found. The difference of 16 mass units could be explained by the formal loss of one oxygen atom. Such a reaction could occur *via* the abstraction of one OH$^\bullet$, followed by subsequent H$^\bullet$ addition, albeit the reaction pathway can be more complex. The calculated *m/z* ratios for such reaction products are in very good agreement with measured *m/z* ratios and was also observed in the radiolysis of C5-BPP (Wilden et al., 2016). The mass spectra shown in Fig. 3 showed the most abundant radiolysis products in the range of *m/z* 500–1000 for better visibility. The only identified CyMe$_4$BTBP radiolysis products with lower *m/z* ratios as the parent molecule were found to be 6'-(5,5,8,8-tetramethyl-5,6,7,8-tetrahydrobenzo[e][1,2,4]-triazin-3-yl)-[2,2′-bipyridine]-6-carbonitrile and [2,2′-bipyridine]-6,6′-dicarbonitrile ("Carbonitrile" and "Dicarbonitrile" in Table 3, see also Fig. S6). The carbonitrile has been observed before by Fermvik et al. for the radiolysis of CyMe$_4$BTBP in cyclohexanone and 1-hexanol (Fermvik, 2011), and Nicolas et al. for the hydrolysis of CyMe$_4$BTBP (Nicolas et al., 2011). The dicarbonitrile was found only in extremely small amounts. Comparable compounds were found for the radiolysis of CyMe$_4$BTPhen in very small amounts as well (Table 4, see also Fig. S7). All identified molecules and ligand fragments are summarized in Tables 3 and 4 for CyMe$_4$BTBP and CyMe$_4$BTPhen, respectively.

Figs. S8 and S9 show proposed reaction schemes for the radiolysis of CyMe$_4$BTBP and CyMe$_4$BTPhen, respectively, summarizing the different reactions described in this paper. We were not able yet to determine the molecular structures of the addition products. Irradiation experiments using ligand solutions in deuterated 1-octanol and subsequent ^{1}H and ^{13}C-NMR analyses were not successful. Afsar et al. synthesized chloro- and bromo-CyMe$_4$BTBP with the addition of the halides in 4-position of the pyridine ring, which were able to extract trivalent metal ions (Afsar et al., 2016). Therefore, we chose to show the radical addition products substituted at this position in Figs. S8 and S9, although the exact structure is unknown. The substitution in 4-position of the pyridine ring would also explain the preservation of the extraction properties as discussed above.

Fig. 4 shows exemplary mass spectra of CyMe$_4$BTBP and CyMe$_4$BTPhen solutions irradiated to 132 kGy in contact with 1.0 mol L^{-1} nitric acid (all mass spectra are shown in Figure S2 to Figs. S2–S5). In principle, the same peaks were found as for the samples irradiated without nitric acid contact (Fig. 3), but with generally higher intensities of the parent molecule species (M+H$^+$). The addition products were similarly observed, but in contrast to the samples irradiated without acid contact, the M+1OctOH addition products were mainly found in the unreduced form. The reduced forms (+2H) were only found in traces. Higher addition products with two α-hydroxyoctyl radicals added (M+2OctOH) were present in lower intensities, for CyMe$_4$BTBP interestingly predominantly in the reduced form, while for CyMe$_4$BTPhen mainly in the unreduced form. The *n*-heptyl and 8-hydroxypentadecanyl radical addition products were found with low intensities. 1-Octanol is known to extract considerable amounts of water and nitric acid when equilibrated with nitric acid solutions (Lang, 2012; Woodhead et al., 2019). The considerably lower formation of radiolysis products is therefore attributed to the scavenging of reactive radicals in the organic phase by extracted water and nitric acid (Horne et al., 2020). Therefore, contact with aqueous nitric acid solution during irradiation has a protective effect, especially on CyMe$_4$BTBP. This confirms the observations from the solvent extraction experiments and will be described more quantitatively in the following discussion.

3.3. (Semi-) quantification of radiolysis products

Quantitative analyses of irradiated samples were carried out to measure the decrease in ligand concentration as a function of absorbed dose. Freshly prepared solutions of 10 mmol L^{-1} CyMe$_4$BTBP or CyMe$_4$BTPhen in 1-octanol were used for calibration and as references. Fig. 5 shows the measured ligand concentrations in organic solutions irradiated without and with contact to 0.1 and 1.0 mol L^{-1} nitric acid as a function of the absorbed dose from HPLC-MS. The data shows some

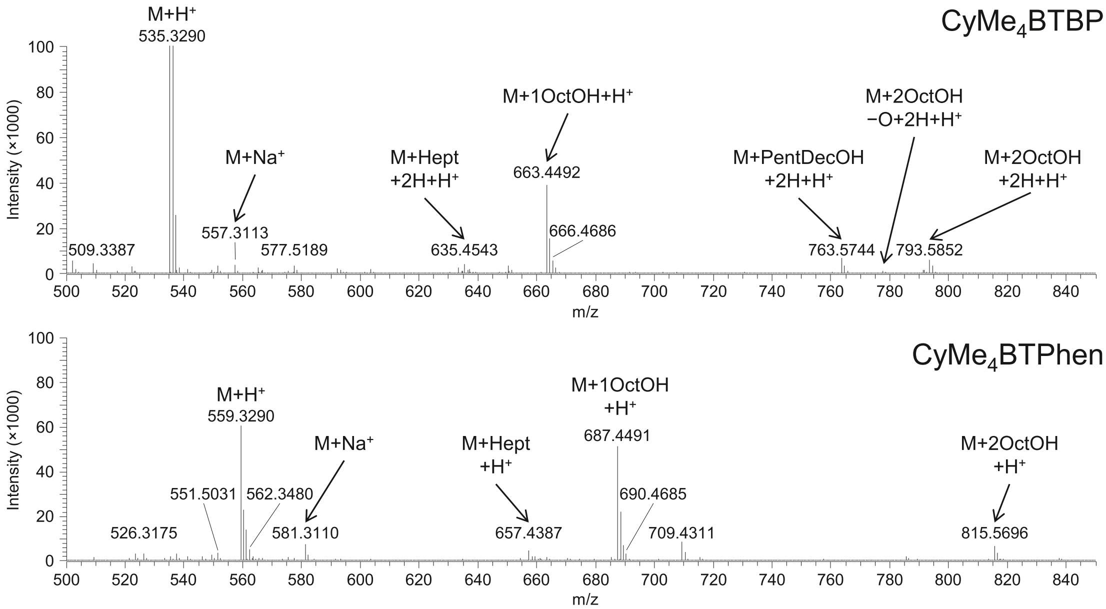

Fig. 4. Mass spectra of 10 mmol L^{-1} CyMe$_4$BTBP (top) and CyMe$_4$BTPhen (bottom) in 1-octanol irradiated to 132 kGy absorbed dose in contact with 1.0 mol L^{-1} nitric acid. M = CyMe$_4$BTBP or CyMe$_4$BTPhen, OctOH = α-hydroxyoctyl, PentDecOH = 8-hydroxypentadecanyl, Hept = heptyl.

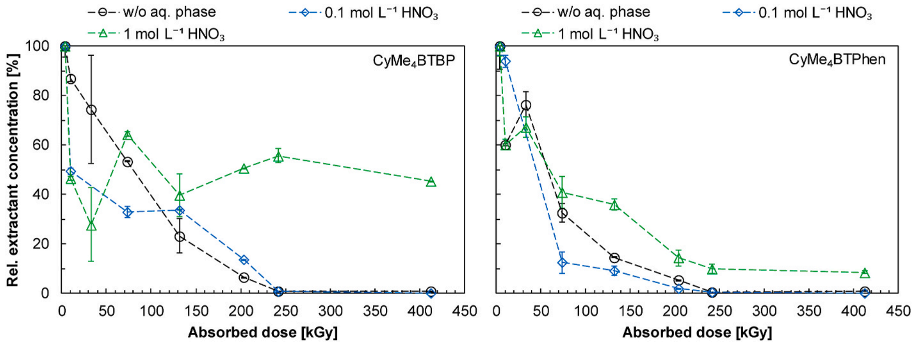

Fig. 5. Decrease of the CyMe$_4$BTBP (left) and CyMe$_4$BTPhen (right) concentration as a function of the absorbed dose. Data is normalized to the measured concentration in the unirradiated sample. 10 mmol L^{-1} solutions of CyMe$_4$BTBP and CyMe$_4$BTPhen in 1-octanol were irradiated without and with contact to 0.1 and 1.0 mol L^{-1} HNO$_3$ and analyzed by HPLC HR-MS.

scattering but generally compares well with additional data obtained from direct infusion mass spectrometry (not shown) (Schmidt et al., 2016). For solutions irradiated without contact to nitric acid a steep decrease in the remaining ligand concentration was observed. This is in good agreement with results from solvent extraction, assuming the observed decreasing distribution ratios resulting from the decreasing concentration of the ligand molecules (Fig. 2). The ligand degradation without acid contact occurred within the same dose range for both ligands. After 250 kGy absorbed dose, the remaining CyMe$_4$BTBP and CyMe$_4$BTPhen concentrations were below the detection limit. For the organic solutions irradiated in contact with 0.1 mol L^{-1} HNO$_3$, no protective effect was found. In contrast, degradation of both ligands seemed to be even higher under these conditions. This is contradictory to the solvent extraction results, where higher distribution ratios were observed when the solvents were irradiated in contact with 0.1 mol L^{-1} HNO$_3$. For irradiation of the organic phases in contact with 1.0 mol L^{-1} nitric acid, higher final ligand concentrations were found up to 413 kGy absorbed dose. For CyMe$_4$BTBP, the final concentration was nearly 45%, while in the case of CyMe$_4$BTPhen roughly 10% of the initial ligand concentration remained. In comparison with results from solvent extraction, the low ligand concentration of CyMe$_4$BTPhen was surprising, since high americium distribution ratios were found for both ligands after radiolysis (Fig. 2).

As the parent molecule concentrations decreased with increasing

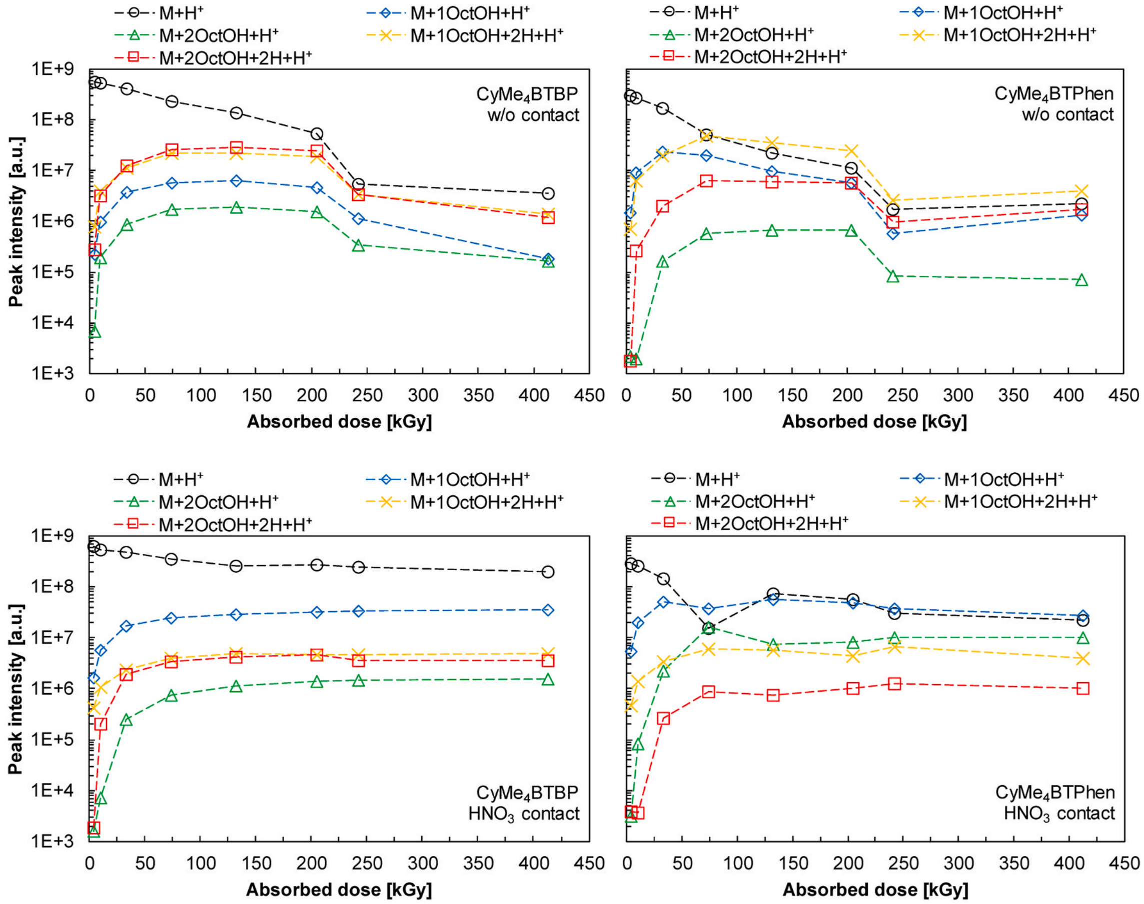

Fig. 6. Peak intensities of the parent molecules and the radiolysis products as a function of the absorbed dose for CyMe$_4$BTBP (left) and CyMe$_4$BTPhen (right), irradiated without contact to an aqueous phase (top) or in contact with 1.0 mol L^{-1} HNO$_3$ (bottom). Measured *m/z* ratios of the fragments are given in Tables 3 and 4.

absorbed dose, but An^{3+} extraction was nearly not influenced, our previous assumption that at least one of the observed radiolytic addition products is also capable of extracting An^{3+} is confirmed. Similar observations were made by Fermvik (2011). The ligand concentration after radiolysis and calculated theoretical americium distribution ratios were determined and compared with measured *D* values. The values for cyclohexanone were in good agreement, but for 1-hexanol higher distribution ratios were observed than calculated based on the remaining ligand concentration. In subsequent mass spectrometric measurements, addition products of up to three solvent molecules to $CyMe_4BTBP$ were found, comparable with our findings.

The quantification of radiolysis products in irradiated samples was not possible directly, as analytical standards were not available. Instead, the measured intensities of the mass spectrometric runs were interpreted. Fig. 6 shows the results of these semi-quantitative measurements of the ligand molecules and the addition products of one and two α-hydroxyoctyl radicals (M+1OctOH and M+2OctOH) as a function of the absorbed dose for $CyMe_4BTBP$ and $CyMe_4BTPhen$ solutions irradiated without contact to an aqueous phase or in contact with 1.0 mol L^{-1} HNO_3. The quantitative measurements and semi quantification results using HR-MS intensities were in good agreement for the parent molecules (the $M+H^+$ *m/z* intensities). Without contact to an aqueous phase (Fig. 6, top) a quick decrease in the parent molecule peak intensities over several orders of magnitude was observed, comparable to the quantitative measurements shown in Fig. 5. The radiolysis products' intensities increase to a maximum at ca. 200 kGy after which their intensities decrease with higher doses. In contrast, radiolytic degradation of $CyMe_4BTBP$ and $CyMe_4BTPhen$, as well as degradation of the radiolysis products themselves is reduced significantly by 1.0 mol L^{-1} nitric acid contact during irradiation (Fig. 6, bottom). After a slight initial degradation of the ligand molecules and buildup of the addition products, the intensities of the ligand molecules as well as the M+1OctOH and M+2OctOH addition products remain relatively constant up to 400 kGy. The semi-quantification data again suggests a higher stability of $CyMe_4BTBP$ compared to $CyMe_4BTPhen$ under these conditions, as $CyMe_4BTPhen$ peak intensities further decrease with increasing dose.

3.4. Steady state pulse radiolysis

Solvated electrons were generated in 1-octanol solution containing 2.5, 5.0, 7.5 and 10.0 mmol L^{-1} $CyMe_4BTBP$ and $CyMe_4BTPhen$, respectively, and their lifetime and subsequent reaction with the ligand molecules following equation (5) was recorded. The results in Fig. 7 show that for both ligands, a faster reaction rate (faster decrease in absorbance) was detected with increasing ligand concentration. This is attributed to an increasing reaction rate of solvated electrons with the ligand molecules. Second-order rate constants (k) were calculated from the slopes in Fig. 7 and found to be $(1.60 \pm 0.04) \times 10^9$ L mol^{-1} s^{-1} for $CyMe_4BTBP$ and $(1.05 \pm 0.03) \times 10^9$ L mol^{-1} s^{-1} for $CyMe_4BTPhen$.

These results imply that both ligands react rapidly with the solvated electron according to equation (5) and that $CyMe_4BTBP$ reacts faster than $CyMe_4BTPhen$. Molecular orbital calculations by Szreder et al. showed that the excess electron is delocalized within the structure of the $CyMe_4BTPhen$ radical anion with the highest electron density on the triazinyl moieties, which contribute in stabilizing the system (Szreder et al., 2019). Additionally, no fragmentation of the molecule was observed and it was concluded that the radical anion has a relatively long life-time and is able to undergo further reactions. Szreder et al. measured a rate constant of $(1.85 \pm 0.09) \times 10^9$ L mol^{-1} s^{-1} for the reaction of $CyMe_4BTPhen$ with the solvated electron in 1-octanol, which is in good agreement with our results (Szreder et al., 2019). Further steady-state irradiation experiments under oxidizing and reducing conditions are planned in the future to clarify the role of solvated electrons in molecule degradation. To study the role of water and nitric acid during radiolysis, steady state pulse radiolysis experiments were conducted using solutions of 2.5–10.0 mmol L^{-1} $CyMe_4BTPhen$ in pure dried 1-octanol as well as in 1-octanol previously contacted with 6.0 mol L^{-1} nitric acid. The absorbance of the solvated electrons was monitored as a function of time (Fig. 8). For samples containing only the ligand molecule and 1-octanol, a clear absorbance of solvated electrons was found, whereas the acid contacted 1-octanol solvent did not show an absorbance of solvated electrons. In contrast to equation (5), where the solvated electrons were captured by ligand molecules forming ligand radical anions, in the presence of dissociated nitric acid the solvated electrons are captured by protons or nitrate anions to form hydrogen atoms (equation (3)) and other transient species. Due to this process, fewer solvated electrons are available to directly form ligand radical anions.

Analysis of the new absorbance kinetics under these contacted acidic octanol conditions was also performed, as shown in Fig. 8. The measured absorbance profiles were fitted to a standard pseudo-first-order growth and decay function, with the growth component value plotted against the ligand concentration (Fig. 8, Bottom Left and Bottom Right) to obtain the second-order rate constants for hydrogen atom ($H^\bullet$) reaction

$$CyMe_4BTPhen + H^\bullet \rightarrow [CyMe_4BTPhenH]^\bullet \quad (6)$$

as $k_6 = (3.18 \pm 0.08) \times 10^8$ L mol^{-1} s^{-1} and $(4.16 \pm 0.06) \times 10^8$ L mol^{-1} s^{-1} for $CyMe_4BTBP$ and $CyMe_4BTPhen$, respectively.

4. Conclusions

The gamma radiolysis of $CyMe_4BTBP$ and $CyMe_4BTPhen$ in 1-octanol solution with and without contact with nitric acid was studied comparatively to examine the influence of structural changes in the ligand backbone on the radiolytic stability. Solvent extraction experiments showed that irradiation of the pure solvent lead to a rapid decrease in distribution ratios of the tested trivalent actinide and lanthanide ions (Am^{3+}, Cm^{3+}, Eu^{3+}) for both ligands, and an almost

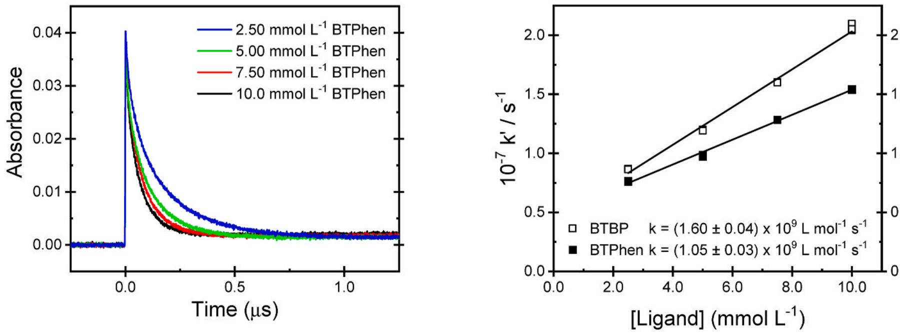

Fig. 7. Left: Decay kinetics of the solvated electron in 1-octanol at 640 nm for different concentrations of $CyMe_4BTPhen$. Right: Calculated second-order rate constants for solvated electron reaction with $CyMe_4BTBP$ and $CyMe_4BTPhen$ as obtained from fitting pseudo-first-order kinetics to the observed decay data for the different ligand concentrations in 1-octanol (cf. equation (5)).

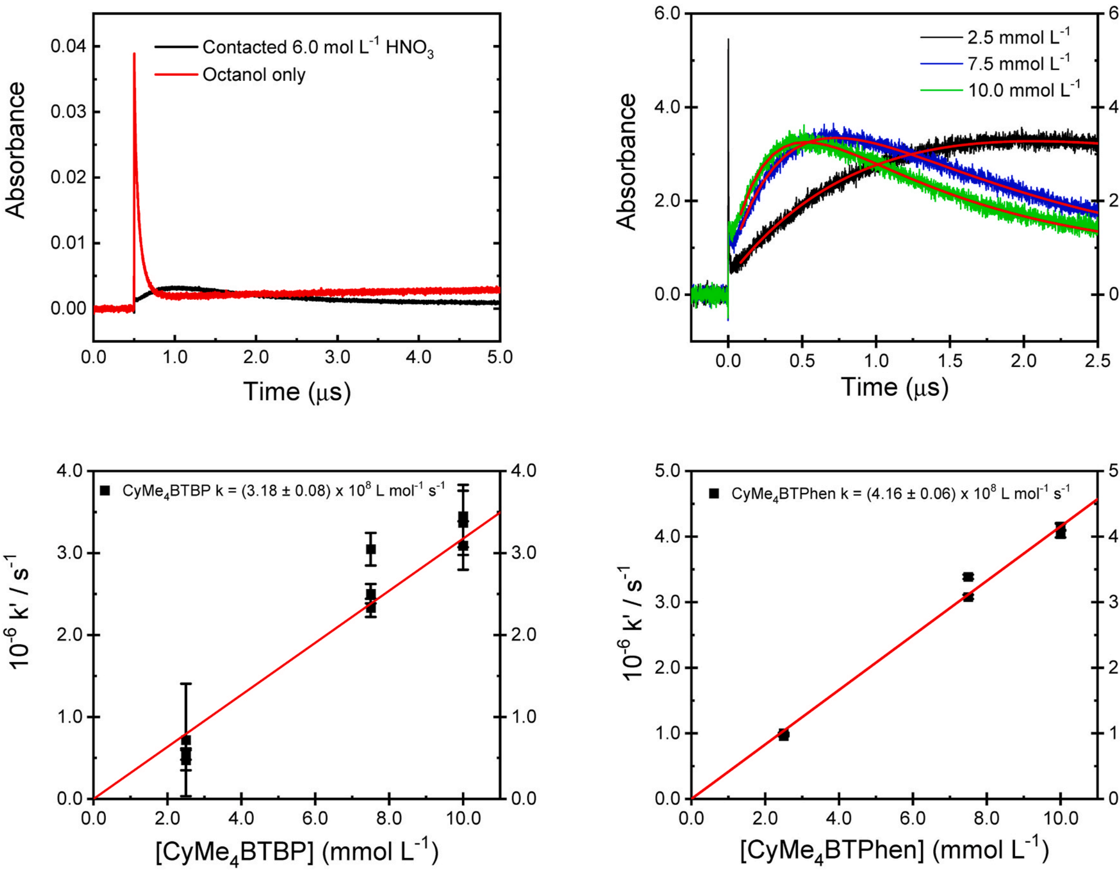

Fig. 8. Top Left: Absorbance decays of the solvated electron in the presence of 10.0 mmol L^{-1} $CyMe_4BTPhen$ in pure 1-octanol (red) and 1-octanol contacted with 6.0 mol L^{-1} HNO_3 (black). **Top Right**: $CyMe_4BTPhen$ concentration dependence of the new growth following solvated electron decay observed at 640 nm. Solid red lines are calculated fits using a pseudo-first-order growth and decay kinetic model. **Bottom Left**: Second-order rate constant determination for $H^•$ atom reaction with $CyMe_4BTBP$ in 1-octanol, with calculated rate constant of $k = (3.18 \pm 0.08) \times 10^8$ L mol^{-1} s^{-1}. **Bottom Right**: Second-order rate constant determination for $H^•$ atom reaction with $CyMe_4BTPhen$ in 1-octanol, with calculated rate constant of $k = (4.16 \pm 0.06) \times 10^8$ L mol^{-1} s^{-1}. (For interpretation of the references to colour in this figure legend, the reader is referred to the Web version of this article.)

complete loss of extraction at 200–300 kGy absorbed dose. Irradiation of the solvents in contact with nitric acid solution showed a stabilization ($CyMe_4BTBP$), or even an increase ($CyMe_4BTPhen$) of the metal ion distribution ratios and preservation of the high selectivity of the extractants. This is attributed to the formation of radiolysis products that are good An^{3+} extractants with high selectivity themselves. Radiolysis products were identified by high-resolution mass spectrometric analyses. Comparable radiolysis products were found for both ligands, mainly formed through addition of diluent radicals formed by prior reaction of diluent molecules with the incident gamma radiation, following an indirect radiolysis mechanism. Although no direct information on the location of the addition site of the α-hydroxyoctyl and other radicals to the ligand molecule is available from the mass spectrometric measurements, the retention of good extraction properties of solvents irradiated in contact with nitric acid implies a substitution in the outer region of the ligand backbones, *i.e.* outside the binding cleft which accommodates the target metal ion. Quantification of the remaining ligand concentrations in irradiated solvents and semi quantification of radiolysis products further fortified that assumption. The quantification showed that the $CyMe_4BTBP$ concentrations after receiving a certain dose were higher than the $CyMe_4BTPhen$ concentrations, and hence $CyMe_4BTBP$ can be considered more stable against radiolysis. However, from an applications point of view, a solvent extraction process might be operated longer with $CyMe_4BTPhen$, as metal ion distribution ratios are higher after the same dose than for $CyMe_4BTBP$. Further irradiation experiments employing loop radiolysis tests in a continuous operation mode will be necessary to finally decide which ligand could be better used in the hydrometallurgical treatment of used nuclear fuel. Steady state pulse radiolysis experiments showed that the solvated electron presumably is the main reactive species in the radiolysis of $CyMe_4BTBP$ and $CyMe_4BTPhen$ in 1-octanol. When solvents were irradiated in contact with nitric acid, solvated electrons were preferentially captured by nitric acid instead of reacting with the ligands or the 1-octanol diluent, resulting in a partial protection of the ligand molecules. Our future research aims at better understanding the observed protective effect of nitric acid. Additionally, the molecular structures of the formed addition products must be clarified. This will also enable the development of improved extractants with enhanced radiation stability and better extraction properties.

CRediT authorship contribution statement

Holger Schmidt: Conceptualization, Formal analysis, Investigation, Methodology, Project administration, Validation, Visualization, Writing – original draft, Writing – review & editing. **Andreas Wilden:** Conceptualization, Formal analysis, Investigation, Methodology, Project administration, Supervision, Validation, Visualization, Writing – original draft, Writing – review & editing. **Giuseppe Modolo:** Conceptualization, Funding acquisition, Project administration, Resources, Supervision, Writing – review & editing. **Dirk Bosbach:** Conceptualization, Funding acquisition, Resources, Supervision, Writing – review & editing. **Beatrix Santiago-Schübel:** Formal analysis, Investigation, Methodology, Resources, Validation, Writing – review & editing. **Michelle Hupert:** Formal analysis, Investigation, Methodology, Validation, Writing – review & editing. **Bruce J. Mincher:** Conceptualization, Formal analysis, Investigation, Methodology, Resources, Validation, Writing – review & editing. **Stephen P. Mezyk:** Conceptualization, Formal analysis, Investigation, Methodology, Resources, Validation, Visualization, Writing – original draft, Writing – review & editing. **Jaroslav Švehla:** Formal analysis, Investigation, Methodology, Validation, Writing – review & editing. **Bohumir Grüner:** Formal analysis, Funding acquisition, Investigation, Methodology, Resources, Validation, Writing – review & editing. **Christian Ekberg:** Funding acquisition, Methodology, Resources, Validation, Writing – review & editing, All authors have read and agreed to the published version of the manuscript.

Declaration of competing interest

The authors declare that they have no known competing financial interests or personal relationships that could have appeared to influence the work reported in this paper.

Acknowledgements

Financial support for this research was provided by the German Federal Ministry of Education and Research (Contract No. 02NUK059D) and the European Commission from the European Atomic Energy Community's 7th Framework program project SACSESS – grant agreement No. FP7-Fission-2012-323-282 and by the H2020 Euratom Research and Innovation Programme under grant agreement n°755171 (project GENIORS). The research used resources of the Brookhaven National Laboratory Laser-Electron Accelerator Facility of the BNL Accelerator Center for Energy Research, also supported by the US-DOE Office of Basic Energy Sciences, Division of Chemical Sciences, Geosciences, and Biosciences under contract DE-SC0012704.

Appendix A. Supplementary data

Supplementary data to this article can be found online at https://doi.org/10.1016/j.radphyschem.2021.109696.

References

Afsar, A., Distler, P., Harwood, L.M., John, J., Westwood, J., 2016. Synthesis and Screening of Modified 6,6'-Bis(5,5,8,8-tetramethyl-5,6,7,8-tetrahydrobenzo[*e*]1,2,4 triazin-3-yl) -2,2'-bipyridine Ligands for Actinide and Lanthanide Separation in Nuclear Waste Treatment. J. Org. Chem. 81 (21), 10517–10520. https://doi.org/10.1021/acs.joc.6b01264.

Aneheim, E., Ekberg, C., Fermvik, A., Foreman, M.R.S.J., Retegan, T., Skarnemark, G., 2010. A TBP/BTBP-based GANEX separation process. Part 1: feasibility. Solvent Extr. Ion Exch. 28 (4), 437–458. https://doi.org/10.1080/07366299.2010.480930.

Aneheim, E., Ekberg, C., Fermvik, A., Foreman, M.R.S.J., Grűner, B., Hájková, Z., Kvičalová, M., 2011. A TBP/BTBP-based GANEX separation process - Part 2: ageing, hydrolytic, and radiolytic stability. Solvent Extr. Ion Exch. 29 (2), 157–175. https://doi.org/10.1080/07366299.2011.539462.

Aneheim, E., Bauhn, L., Ekberg, C., Foreman, M., Lofstrom-Engdahl, E., 2012a. Extraction experiments after radiolysis of a proposed GANEX solvent - the effect of time. Proc. Chem. 7, 123–129. https://doi.org/10.1016/j.proche.2012.10.022.

Aneheim, E., Ekberg, C., Foreman, M.R.S., Löfström-Engdahl, E., Mabile, N., 2012b. Studies of a solvent for GANEX applications containing CyMe$_4$-BTBP and DEHBA in cyclohexanone. Separ. Sci. Technol. 47 (5), 663–669. https://doi.org/10.1080/01496395.2011.627908.

Aneheim, E., Ekberg, C., Foreman, M.R.S., 2013. A TBP/BTBP-Based GANEX separation process – Part 3: fission product handling. Solvent Extr. Ion Exch. 31 (3), 237–252. https://doi.org/10.1080/07366299.2012.757158.

Authen, T.L., Wilden, A., Halleröd, J., Schneider, D., Kreft, F., Modolo, G., Ekberg, C., 2021. Batch tests for optimisation of solvent composition and process flexibility of the CHALMEX FS-13 process. Solvent Extr. Ion Exch. 39 (1), 1–17. https://doi.org/10.1080/07366299.2020.1797988.

Berthon, L., Paquet, A., Saint-Louis, G., Guilbaud, P., 2021. How phase modifiers disrupt third-phase formation in solvent extraction solutions. Solvent Extr. Ion Exch. 39 (2), 204–232. https://doi.org/10.1080/07366299.2020.1831782.

Bjergbakke, E., 1970. The ferrous-cupric dosimeter. In: Holm, N.W., Berry, R.J. (Eds.), Manual on Radiation Dosimetry. Marcel Dekker Inc., New York, pp. 319–321.

Buxton, G.V., Greenstock, C.L., Helman, W.P., Ross, A.B., 1988. Critical review of rate constants for reactions of hydrated electrons, hydrogen atoms and hydroxyl radicals ($^{\cdot}$OH/$^{\cdot}$O^{-}) in aqueous solution. J. Phys. Chem. Ref. Data 17 (2), 513–886. https://doi.org/10.1063/1.555805.

Distler, P., Kondé, J., John, J., Hájková, Z., Švehla, J., Grüner, B., 2015. Characterization of solvents containing CyMe$_4$-BTPhen in selected cyclohexanone-based diluents after irradiation by accelerated electrons. Nukleonika 60, 4 (Pt. II), 885–891. https://doi.org/10.1515/nuka-2015-0123.

Ekberg, C., Fermvik, A., Retegan, T., Skarnemark, G., Foreman, M.R.S., Hudson, M.J., Englund, S., Nilsson, M., 2008. An overview and historical look back at the solvent extraction using nitrogen donor ligands to extract and separate An(III) from Ln(III). Radiochim. Acta 96 (4–5 EUROPART), 225–233. https://doi.org/10.1524/ract.2008.1483.

Fermvik, A., 2011. Radiolytic Degradation of BTBP Type Molecules for Treatment of Used Nuclear Fuel by Solvent Extraction. Chalmers University, Gothenburg, Sweden.

Fermvik, A., Berthon, L., Ekberg, C., Englund, S., Retegan, T., Zorz, N., 2009. Radiolysis of solvents containing C5-BTBP: identification of degradation products and their dependence on absorbed dose and dose rate. Dalton Trans. 32, 6421–6430. https://doi.org/10.1039/b907084b.

Fermvik, A., Nilsson, M., Ekberg, C., 2010. Radiolytic degradation of heterocyclic nitrogen containing ligands from low dose-rate gamma sources. In: Wai, C.M., Mincher, B.J. (Eds.), Nuclear Energy and the Environment, vol. 1046. American Chemical Society, Washington, pp. 215–229.

Fermvik, A., Grüner, B., Kvíčalová, M., Ekberg, C., 2011. Semi-quantitative and quantitative studies on the gamma radiolysis of C5-BTBP. Radiochim. Acta 99 (2), 113–119. https://doi.org/10.1524/ract.2011.1800.

Fermvik, A., Aneheim, E., Grüner, B., Hájková, Z., Kvicalová, M., Ekberg, C., 2012. Radiolysis of C5-BTBP in cyclohexanone irradiated in the absence and presence of an aqueous phase. Radiochim. Acta 100 (4), 273–282. https://doi.org/10.1524/ract.2012.1908.

Freeman, G.R., 1970. Radiolysis of alcohols. Actions Chim. Biol. Radiat. 14, 73–134.

Geist, A., 2010. Extraction of nitric acid into alcohol: kerosene mixtures. Solvent Extr. Ion Exch. 28 (5), 596–607. https://doi.org/10.1080/07366299.2010.499286.

Geist, A., Modolo, G., September, 2009. TODGA process development: an improved solvent formulation. In: Proceedings of GLOBAL (The Nuclear Fuel Cycle: Sustainable Options & Industrial Perspectives): Paris, 2009, vols. 6–11, pp. 1022–1026 paper 9193.

Geist, A., Panak, P.J., 2021. Recent progress in trivalent actinide and lanthanide solvent extraction and coordination Chemistry with triazinylpyridine N donor ligands. Solvent Extr. Ion Exch. 39 (2), 128–151. https://doi.org/10.1080/07366299.2020.1831235.

Geist, A., Hill, C., Modolo, G., Foreman, M.R.S.J., Weigl, M., Gompper, K., Hudson, M.J., Madic, C., 2006. 6,6'-Bis(5,5,8,8-tetramethyl-5,6,7,8-tetrahydro-benzo[1,2,4] triazin-3-yl)[2,2']bipyridine, an effective extracting agent for the separation of americium(III) and curium(III) from the lanthanides. Solvent Extr. Ion Exch. 24 (4), 463–483. https://doi.org/10.1080/07366290600761936.

Geist, A., Adnet, J.-M., Bourg, S., Ekberg, C., Galán, H., Guilbaud, P., Miguirditchian, M., Modolo, G., Rhodes, C., Taylor, R., 2020. An overview of solvent extraction processes developed in Europe for advanced nuclear fuel recycling, Part 1 — heterogeneous recycling. Separ. Sci. Technol. https://doi.org/10.1080/01496395.2020.1795680.

Halleröd, J., Ekberg, C., Löfström-Engdahl, E., Aneheim, E., 2015. Development of the Chalmers grouped actinide extraction process. Nukleonika 60, 4 (Pt. II), 829–835. https://doi.org/10.1515/nuka-2015-0115.

Hill, C., Guillaneux, D., Berthon, L., 2002. SANEX-BTP process development studies. In: Proceedings of 16th International Solvent Extraction Conference, ISEC2002, 17–21 March, 2002, pp. 1205–1209. Cape Town, South Africa.

Hill, C., Berthon, L., Madic, C., October, 2005. Study of the stability of BTP extractants under radiolysis. In: Proceedings of GLOBAL: Tsukuba, Japan, 2005. 9–13, p. 283.

Horne, G.P., Zarzana, C., Rae, C., Cook, A.R., Mezyk, S.P., Zalupski, P., Wilden, A., Mincher, B.J., 2020. Does addition of 1-octanol as a phase modifier provide radical scavenging radioprotection for *N,N,N',N'*-tetraoctyldiglycolamide (TODGA)? Phys. Chem. Chem. Phys. 22 (43), 24978–24985. https://doi.org/10.1039/D0CP04310A.

Hudson, M.J., Boucher, C.E., Braekers, D., Desreux, J.F., Drew, M.G.B., Foreman, M.R.S. J., Harwood, L.M., Hill, C., Madic, C., Marken, F., Youngs, T.G.A., 2006. New bis (triazinyl) pyridines for selective extraction of americium(III). New J. Chem. 30 (8), 1171–1183. https://doi.org/10.1039/b514108g.

Kolarik, Z., Mullich, U., Gassner, F., 1999. Selective extraction of Am(III) over Eu(III) by 2,6-ditriazolyl- and 2,6-ditriazinylpyridines. Solvent Extr. Ion Exch. 17 (1), 23–32. https://doi.org/10.1080/07360299908934598.

Kondé, J., Distler, P., John, J., Švehla, J., Grüner, B., Bělčická, Z., 2016. Radiation influencing of the extraction properties of the CyMe$_4$-BTBP and CyMe$_4$-BTPhen solvents with FS-13. Procedia Chem. 21, 174–181. https://doi.org/10.1016/j.proche.2016.10.025.

Lang, B.E., 2012. Solubility of water in octan-1-ol from (275 to 369) K. J. Chem. Eng. Data 57 (8), 2221–2226. https://doi.org/10.1021/je3001427.

Lewis, F.W., Harwood, L.M., Hudson, M.J., Drew, M.G.B., Desreux, J.F., Vidick, G., Bouslimani, N., Modolo, G., Wilden, A., Sypula, M., Vu, T.-H., Simonin, J.-P., 2011. Highly efficient separation of actinides from lanthanides by a phenanthroline-derived bis-triazine ligand. J. Am. Chem. Soc. 133 (33), 13093–13102. https://doi.org/10.1021/ja203378m.

Lewis, F.W., Harwood, L.M., Hudson, M.J., Drew, M.G.B., Wilden, A., Sypula, M., Modolo, G., Vu, T.-H., Simonin, J.-P., Vidick, G., Bouslimani, N., Desreux, J.F., 2012. From BTBPs to BTPhens: the effect of ligand pre-organization on the extraction properties of quadridentate bis-triazine ligands. Proc. Chem. 7, 231–238. https://doi.org/10.1016/j.proche.2012.10.038.

Lewis, F.W., Harwood, L.M., Hudson, M.J., Drew, M.G.B., Hubscher-Bruder, V., Videva, V., Arnaud-Neu, F., Stamberg, K., Vyas, S., 2013. BTBPs versus BTPhens:

some reasons for their differences in properties concerning the partitioning of minor actinides and the advantages of BTPhens. Inorg. Chem. 52 (9), 4993–5005. https://doi.org/10.1021/ic3026842.

Logunov, M.V., Voroshilov, Y.A., Starovoitov, N.P., Shadrin, A.Y., Smirnov, I.V., Kvasnitskii, I.B., Tananaev, I.G., Myasoedov, B.F., Morgalyuk, V.P., Kamiya, M., Koma, I., Koyama, T., 2006. Radiation resistance of a series of organophosphorus extractants. Radiochemistry 48 (1), 55–61. https://doi.org/10.1134/S1066362206010127.

Magnusson, D., Christiansen, B., Foreman, M.R.S., Geist, A., Glatz, J.P., Malmbeck, R., Modolo, G., Serrano-Purroy, D., Sorel, C., 2009a. Demonstration of a SANEX process in centrifugal contactors using the CyMe$_4$-BTBP molecule on a genuine fuel solution. Solvent Extr. Ion Exch. 27 (2), 97–106. https://doi.org/10.1080/07366290802672204.

Magnusson, D., Christiansen, B., Malmbeck, R., Glatz, J.P., 2009b. Investigation of the radiolytic stability of a CyMe$_4$-BTBP based SANEX solvent. Radiochim. Acta 97 (9), 497–502. https://doi.org/10.1524/ract.2009.1647.

Magnusson, D., Geist, A., Wilden, A., Modolo, G., 2013. Direct selective extraction of actinides (III) from PUREX raffinate using a mixture of CyMe$_4$-BTBP and TODGA as 1-cycle SANEX solvent Part II: flow-sheet design for a counter-current centrifugal contactor demonstration process. Solvent Extr. Ion Exch. 31 (1), 1–11. https://doi.org/10.1080/07366299.2012.700596.

Mezyk, S.P., Mincher, B.J., Dhiman, S.B., Layne, B., Wishart, J.F., 2016. The role of organic solvent radical cations in separations ligand degradation. J. Radioanal. Nucl. Chem. 307 (3), 2445–2449. https://doi.org/10.1007/s10967-015-4582-7.

Mincher, B.J., Mezyk, S.P., 2009. Radiation chemical effects on radiochemistry: a review of examples important to nuclear power. Radiochim. Acta 97 (9), 519–534. https://doi.org/10.1524/ract.2009.1646.

Mincher, B.J., Arbon, R.E., Knighton, W.B., Meikrantz, D.H., 1994. Gamma-ray-induced degradation of PCBs in neutral isopropanol using spent reactor-fuel. Appl. Radiat. Isot. 45 (8), 879–887. https://doi.org/10.1016/0969-8043(94)90219-4.

Mincher, B.J., Modolo, G., Mezyk, S.P., 2009. Review article: the effects of radiation Chemistry on solvent extraction: 1. Conditions in acidic solution and a review of TBP radiolysis. Solvent Extr. Ion Exch. 27 (1), 1–25. https://doi.org/10.1080/07366290802544767.

Mincher, B.J., 2010a. An overview of selected radiation chemical reactions affecting fuel cycle solvent extraction. Chap. 15. In: Wai, C.M., Mincher, B.J. (Eds.), Nuclear Energy and the Environment, vol. 1046. American Chemical Society, pp. 181–192.

Mincher, B.J., Modolo, G., Mezyk, S.P., 2010b. Review: the effects of radiation Chemistry on solvent extraction 4: separation of the trivalent actinides and considerations for radiation-resistant solvent systems. Solvent Extr. Ion Exch. 28 (4), 415–436. https://doi.org/10.1080/07366299.2010.485548.

Modolo, G., Wilden, A., Daniels, H., Geist, A., Magnusson, D., Malmbeck, R., 2013. Development and demonstration of a new SANEX partitioning process for selective actinide(III)/Lanthanide(III) separation using a mixture of CyMe$_4$BTBP and TODGA. Radiochim. Acta 101 (3), 155–162. https://doi.org/10.1524/ract.2013.2016.

Modolo, G., Wilden, A., Kaufholz, P., Bosbach, D., Geist, A., 2014. Development and demonstration of innovative partitioning processes (i-SANEX and 1-cycle SANEX) for actinide partitioning. Prog. Nucl. Energy 72, 107–114. https://doi.org/10.1016/j.pnucene.2013.07.021.

Modolo, G., Geist, A., Miguirditchian, M., 2015. Minor actinide separations in the reprocessing of spent nuclear fuels: recent advances in Europe. Chap. 10. In: Taylor, R. (Ed.), Reprocessing and Recycling of Spent Nuclear Fuel. Woodhead Publishing, Oxford, pp. 245–287.

Modolo, G., Sypula, M., Geist, A., Hill, C., Sorel, C., Malmbeck, R., Magnusson, D., Foreman, M.R.S.J., October, 2008. Development and demonstration of a new SANEX-process for actinide(III)/Lanthanide(III) separation using a mixture of CyMe$_4$BTBP and TODGA as selective extractant. In: Proceedings of 10th Information Exchange Meeting on Actinide and Fission Product Partitioning and Transmutation: Mito, Japan, 2008, vols. 6–10, pp. 235–241.

Nicolas, G., Jankowski, C.K., Lucas-Lamouroux, C., Bresson, C., 2011. Development of normal phase-high performance liquid chromatography-atmospherical pressure chemical ionization-mass spectrometry method for the study of 6,6 ’-bis-(5,5,8,8-tetramethyl-5,6,7,8-tetrahydro-benzo 1,2,4 -triazin-3-yl)- 2,2 ’ -bipyridine hydrolytic degradation. J. Chromatogr. A 1218 (37), 6369–6378. https://doi.org/10.1016/j.chroma.2011.07.003.

Nilsson, M., Andersson, S., Ekberg, C., Foreman, M.R.S., Hudson, M.J., Skarnemark, G., 2006. Inhibiting radiolysis of BTP molecules by addition of nitrobenzene. Radiochim. Acta 94 (2), 103–106. https://doi.org/10.1524/ract.2006.94.2.103.

OECD-NEA *Potential Benefits and Impacts of Advanced Nuclear Fuel Cycles with Actinide Partitioning and Transmutation*, 2011. OECD, Nuclear Energy Agency (NEA).

Panak, P.J., Geist, A., 2013. Complexation and extraction of trivalent actinides and lanthanides by triazinylpyridine N-donor ligands. Chem. Rev. 113 (2), 1199–1236. https://doi.org/10.1021/cr3003399.

Poinssot, C., Bourg, S., Boullis, B., 2016. Improving the nuclear energy sustainability by decreasing its environmental footprint. Guidelines from life cycle assessment simulations. Prog. Nucl. Energy 92, 234–241. https://doi.org/10.1016/j.pnucene.2015.10.012.

Retegan, T., Ekberg, C., Englund, S., Fermvik, A., Foreman, M.R.S., Skarnemark, G., 2007. The behaviour of organic solvents containing C5-BTBP and CyMe$_4$-BTBP at low irradiation doses. Radiochim. Acta 95 (11), 637–642. https://doi.org/10.1524/ract.2007.95.11.637.

Schmidt, H., Wilden, A., Modolo, G., Švehla, J., Grüner, B., Ekberg, C., 2015. Gamma radiolytic stability of CyMe$_4$BTBP and effect of nitric acid. Nukleonika 60, 4 (Pt. II), 879–884. https://doi.org/10.1515/nuka-2015-0156.

Schmidt, H., Wilden, A., Modolo, G., Bosbach, D., Santiago-Schübel, B., Hupert, M., Švehla, J., Grüner, B., Ekberg, C., 2016. Gamma radiolysis of the highly selective ligands CyMe$_4$BTBP and CyMe$_4$BTPhen: qualitative and quantitative investigation of radiolysis products. Procedia Chem. 21, 32–37. https://doi.org/10.1016/j.proche.2016.10.005.

Seidl, R., Flüeler, T., Krütli, P., 2021. Sharp discrepancies between nuclear and conventional toxic waste: technical analysis and public perception. J. Hazard Mater. 414, 125422. https://doi.org/10.1016/j.jhazmat.2021.125422.

Serp, J., Poinssot, C., Bourg, S., 2017. Assessment of the anticipated environmental footprint of future nuclear energy systems. Evidence of the beneficial effect of extensive recycling. Energies 10 (9), 1445. https://doi.org/10.3390/en10091445.

Sugo, Y., Sasaki, Y., Tachimori, S., 2002. Studies on hydrolysis and radiolysis of *N,N,N'*, *N'*-tetraoctyl-3-oxapentane-1,5-diamide. Radiochim. Acta 90 (3), 161–165. https://doi.org/10.1524/ract.2002.90.3_2002.161.

Sugo, Y., Izumi, Y., Yoshida, Y., Nishijima, S., Sasaki, Y., Kimura, T., Sekine, T., Kudo, H., 2007. Influence of diluent on radiolysis of amides in organic solution. Radiat. Phys. Chem. 76 (5), 794–800. https://doi.org/10.1016/j.radphyschem.2006.05.008.

Sulich, A., Grodkowski, J., Mirkowski, J., Kocia, R., 2014. Reactions of ligands from BT(B)P family with solvated electrons and benzophenone ketyl radicals in 1-octanol solutions. Pulse radiolysis study. J. Radioanal. Nucl. Chem. 300 (1), 415–421. https://doi.org/10.1007/s10967-014-3021-5.

Swallow, A.J., 1987. Radiation Chemistry of the liquid state: (2) organic liquids. Chap. 11. In: Farhataziz, Rodgers, Michael A.J. (Eds.), Radiation Chemistry - Principles and Applications. VCH Verlagsgesellschaft mbH, Weinheim, Germany, pp. 351–375.

Symons, M.C.R., Eastland, G.W., 1977. Radiation mechanisms. Part 18. The radiolysis of alcohols: an electron spin resonance study. J. Chem. Res.(S) 254–255.

Szreder, T., Schmidt, H., Modolo, G., 2019. Fast radiation-induced reactions in organic phase of SANEX system containing CyMe$_4$-BTPhen extracting agent. Radiat. Phys. Chem. 164, 108356. https://doi.org/10.1016/j.radphyschem.2019.108356.

Veliscek-Carolan, J., 2016. Separation of actinides from spent nuclear fuel: a review. J. Hazard Mater. 318, 266–281. https://doi.org/10.1016/j.jhazmat.2016.07.027.

Wilden, A., Schreinemachers, C., Sypula, M., Modolo, G., 2011. Direct selective extraction of actinides (III) from PUREX raffinate using a mixture of CyMe$_4$BTBP and TODGA as 1-cycle SANEX solvent. Solvent Extr. Ion Exch. 29 (2), 190–212. https://doi.org/10.1080/07366299.2011.539122.

Wilden, A., Modolo, G., Schreinemachers, C., Sadowski, F., Lange, S., Sypula, M., Magnusson, D., Geist, A., Lewis, F.W., Harwood, L.M., Hudson, M.J., 2013. Direct selective extraction of actinides (III) from PUREX raffinate using a mixture of CyMe$_4$BTBP and TODGA as 1-cycle SANEX solvent Part III: demonstration of a laboratory-scale counter-current centrifugal contactor process. Solvent Extr. Ion Exch. 31 (5), 519–537. https://doi.org/10.1080/07366299.2013.775890.

Wilden, A., Modolo, G., Hupert, M., Santiago-Schübel, B., Löfström-Engdahl, E., Halleröd, J., Ekberg, C., Mincher, B.J., Mezyk, S.P., 2016. Gamma-radiolytic stability of solvents containing C5-BPP (2,6-Bis(5-(2,2-dimethylpropyl)-1*H*-pyrazol-3-yl) pyridine) for actinide(III)/lanthanide(III) separation. Solvent Extr. Ion Exch. 34 (1), 1–12. https://doi.org/10.1080/07366299.2015.1115694.

Wishart, J.F., Cook, A.R., Miller, J.R., 2004. The LEAF picosecond pulse radiolysis facility at brookhaven national laboratory. Rev. Sci. Instrum. 75 (11), 4359–4366. https://doi.org/10.1063/1.1807004.

Woodhead, D., McLachlan, F., Taylor, R., Müllich, U., Geist, A., Wilden, A., Modolo, G., 2019. Nitric acid extraction into a TODGA solvent modified with octanol. Solvent Extr. Ion Exch. 37 (2), 173–190. https://doi.org/10.1080/07366299.2019.1625201.

Yu, C.H., Zhang, J.W., Dai, J., Peng, J., Li, J.Q., Zhai, M.L., 2010. Radiation stability and analysis of radiolysis product of 1-octanol. Acta Phys. - Chim. Sin. 26 (4), 988–992. https://doi.org/10.3866/pku.whxb20100434.

Zhou, H.Y., Ao, Y.Y., Yuan, J., Peng, J., Li, J.Q., Zhai, M.L., 2014. Extraction mechanism and γ-radiation effect on the removal of Eu^{3+} by a novel BTPhen/[C$_n$mim] [NTf$_2$] system in the presence of nitric acid. RSC Adv. 4 (85), 45612–45618. https://doi.org/10.1039/c4ra07662a.

Zsabka, P., Van Hecke, K., Wilden, A., Modolo, G., Hupert, M., Jespers, V., Voorspoels, S., Verwerft, M., Binnemans, K., Cardinaels, T., 2020. Gamma radiolysis of TODGA and CyMe$_4$BTPhen in the ionic liquid tri-*n*-octylmethylammonium nitrate. Solvent Extr. Ion Exch. 38 (2), 212–235. https://doi.org/10.1080/07366299.2019.1710918.